

embedded cluster does not necessarily give better FCO-based predictions.

### Relation to Earlier Work

Messmer and Bennett,<sup>7h</sup> in a seminal paper, examined the FCOs of graphite in an attempt to establish symmetry rules for chemisorption *site* preference. Because they used an 18-carbon-atom embedded cluster to generate the FCOs, they based their arguments on the LFCOs. (Use of a different cluster size would have led to other, presumably less dominating, FCOs, a fact that Messmer and Bennett recognized but did not emphasize.) They examined the phases of the LFCOs and, by relating these to phases of MOs of various types of adsorbing species, proposed rules for predicting which sites (atop, over a bond, etc.) would be favored. Clearly, the philosophy behind that work is similar to our effort to relate pattern preference to the nature of the LFCOs. Indeed, Messmer and Bennett allude to this pattern question as a possible extension of their method.<sup>7h</sup> Their results, like ours, are necessarily approximate because they are predicting the results of integrating over all of *k* space from symmetry arguments at one point. It is also necessary, in both types of study, to mix the degenerate LFCOs of graphite to produce the proper zeroth-order COs for the perturbation analysis. Messmer and Bennett omitted this step.<sup>19</sup> This has the effect of preventing the theoretical surface from responding fully to the shifting about of the chemisorbing species, leading to an artificial enhancement in the predicted stabilities of some sites over others and to incorrect site-preference predictions. Despite criticism of their paper,<sup>19</sup> it contains an idea

of some importance—that LFCOs in surfaces can be used to make qualitative predictions concerning chemisorption.

### Conclusions

The frontier orbital hypothesis, that the relative total electronic energies for a series of related situations are paralleled by the relative frontier orbital energies, works well for hydrogen atoms on graphite *at each point in k space*. However, we have to integrate over all *k* points in the first Brillouin zone to obtain the energy per unit cell. This results in relative energies that are not well represented by any particular frontier crystal orbital. Nevertheless, the prediction based on the *leading* frontier orbitals—that the  $\epsilon$  pattern should be less stable than all the others—is true for the energies per unit cell. Therefore, this one point in *k* space appears to be the most reasonable choice to represent (imperfectly) the integrated results.

Embedded-cluster calculations produce crystal orbital energies at only one *k* point. Since it is apparently best if that *k* point corresponds to the *leading* frontier crystal orbitals, it is important that the embedded-cluster size corresponded to a folded band structure wherein the desired *k* point has ended up at the origin of the *k* vectors.

Simple cluster calculations are inappropriate *for the sort of pattern comparisons considered here*. It is probably much easier to use an embedded cluster or band calculation than to attempt to adjust the shape and size of a simple cluster to overcome inherent deficiencies.

Registry No. H, 12385-13-6; graphite, 7782-42-5.

## Surface Structure of Coadsorbed Benzene and Carbon Monoxide on the Rhodium(111) Single Crystal Analyzed with Low-Energy Electron Diffraction Intensities

M. A. Van Hove,\* R. F. Lin,<sup>†</sup> and G. A. Somorjai

Contribution from the Materials and Molecular Research Division, Lawrence Berkeley Laboratory, and Department of Chemistry, University of California, Berkeley, California 94720. Received August 26, 1985

**Abstract:** The first structural analysis of a molecular coadsorbate system is presented. Mutual reordering and site shifting are found to occur for benzene and CO coadsorbed in a  $(\sqrt{3})$  lattice on Rh(111). This low-energy electron diffraction (LEED) intensity analysis yields the first confirmed hollow-site adsorption of CO on a single-crystal metal surface, with a C–O bond length expanded by  $0.06 \pm 0.05$  Å from the gas phase. The flat-lying benzene is found centered over hcp-type hollow sites with a strong Kekulé-type distortion: C–C bond lengths alternate between  $1.33 \pm 0.15$  and  $1.81 \pm 0.15$  Å (hydrogen positions were not determined). This suggests the possibility of a 1,3,5-cyclohexatriene species being formed. The Rh–C bond length is  $2.35 \pm 0.05$  Å for benzene and  $2.16 \pm 0.04$  Å for CO.

### 1. Introduction

A growing amount of structural information is becoming available on monolayers of aromatic molecules adsorbed on transition-metal surfaces.<sup>1</sup> The main techniques used to obtain such information are high-resolution electron energy loss spectroscopy (HREELS), low-energy electron diffraction (LEED), thermal desorption spectroscopy (TDS), angle-resolved ultraviolet photoemission spectroscopy (ARUPS), and near-edge X-ray absorption fine structure (NEXAFS). We report here on the structure of benzene adsorbed on the Rh(111) single-crystal surface in the presence of coadsorbed carbon monoxide. LEED

intensity analysis and HREELS were the primary techniques used in this study. This is the first structure analysis of a two-molecule adsorption system to yield detailed information on the bonding of both molecules to the metal. The interaction between these coadsorbates shows up both in ordering and in bonding effects: the long-range order depends on the relative coverage (concentration).

<sup>†</sup>Permanent address: Department of Physics, Fudan University, Shanghai, People's Republic of China.

(1) (a) Nyberg, G. L.; Richardson, N. V. *Surf. Sci.* **1979**, *85*, 335. (b) Tsai, M.-C.; Muettterties, E. L. *J. Phys. Chem.* **1982**, *86*, 5067. (c) Mas-sardier, J.; Tardy, B.; Abon, M.; Bertolini, J. C. *Surf. Sci.* **1983**, *126*, 154. (d) Surman, M.; Bare, S. R.; Hofmann, P.; King, D. A. *Surf. Sci.* **1983**, *126*, 349. (e) Avery, N. R. *Surf. Sci.* **1984**, *146*, 363. (f) Koel, B. E.; Crowell, J. E.; Mate, C. M.; Somorjai, G. A. *J. Phys. Chem.* **1984**, *88*, 1988. (g) Newmann, M.; Mack, J. U.; Bertel, E.; Netzer, F. P. *Surf. Sci.* **1985**, *155*, 629.

tration) of the two molecules, and each type of molecule bonds very differently to the metal when coadsorbed than in the absence of the other type of molecule.

Our structural results also aid the understanding of chemical reactions involving aromatic molecules on metals. Examples of such reactions include the cyclization of acetylenes to arenes as catalyzed by organometallics<sup>2</sup> or as catalyzed by metal surfaces, especially Pd(111),<sup>3</sup> and the newly observed reaction of benzene conversion to acetylene.<sup>4</sup>

We previously reported<sup>5</sup> the benzene adsorption geometry for the same system discussed here, Rh(111)-c( $2\sqrt{3} \times 4$ )rect or  $-(\frac{3}{1})$ , also obtained by a LEED intensity analysis (the c( $2\sqrt{3} \times 4$ )rect notation is totally equivalent to the  $(\frac{3}{1})$  matrix notation<sup>6</sup>). However, it was not recognized at the time that CO was coadsorbed in an ordered manner with the benzene and therefore no CO was included in the LEED calculations (the presence of CO was known<sup>7</sup> but assumed unimportant to the benzene ordering). The ordering role of coadsorbed CO for organic monolayers on metal surfaces was established by more recent HREELS and TDS experiments performed in this research group.<sup>8</sup> This finding required a reanalysis of the LEED data, including coadsorbed CO in the calculations. It is found that the optimum benzene structure does not change qualitatively when coadsorbed CO is included in the calculations. Thus, our initial benzene structure<sup>5</sup> is substantially confirmed in this work.

## 2. Structure Analysis

**2.1. LEED Data.** The Rh(111) surface and the adsorption structures were prepared by standard techniques, as detailed in ref 7, while LEED intensities were obtained by the photographic method.<sup>7</sup> In our LEED intensity analysis, we have used intensity-energy ( $I$ - $V$ ) curves for 13 symmetry-inequivalent beams measured at normal incidence of the incoming electrons. These beams are labeled (0,-1), (0,1), ( $\frac{1}{2}, \frac{1}{2}$ ), (0, $\frac{1}{2}$ ), (0,- $\frac{1}{2}$ ), ( $\frac{1}{4}, \frac{1}{2}$ ), ( $-\frac{1}{4}, -\frac{1}{2}$ ), ( $\frac{1}{4}, \frac{1}{4}$ ), ( $\frac{1}{8}, \frac{1}{4}$ ), ( $-\frac{1}{8}, -\frac{1}{4}$ ), ( $\frac{5}{8}, \frac{1}{4}$ ), ( $\frac{1}{8}, \frac{5}{8}$ ), and ( $-\frac{1}{8}, -\frac{5}{8}$ ). Photographs and labeling of the  $(\frac{3}{1})$  pattern are shown in ref. 7. The energy range used for comparison with the theory was  $20 \leq E \leq 150$  eV, yielding a cumulative nondegenerate energy range of 1224 eV. These are the same experimental data described previously.<sup>5</sup>

**2.2. LEED Theory.** In the LEED intensity calculations, we have applied the new approximation method called Beam Set Neglect, described and tested before.<sup>5,9</sup> It allows overlayer unit cells of any size and shape to be treated very efficiently by drastically reducing the number of diffraction beams calculated simultaneously. Intralayer multiple scattering within the adsorbate layer was approximated as follows in the new set of calculations (hydrogen is ignored as before). While all internal multiple scattering was included within individual molecules (by use of reverse scattering perturbation and matrix inversion<sup>10</sup>), we ignored all intralayer multiple scattering between molecules. The latter method is particularly efficient, since it can be cast in the form of a simple kinematic summation of the beam scattering properties of the benzene overlayer and of the carbon monoxide overlayer taken separately (we call this "kinematic sublayer addition" or

KSLA). A benefit of this approach is that many different relative positions of the inequivalent molecules can also be obtained efficiently: the only computational step that must be repeated is the economical stacking of layers by renormalized forward scattering.<sup>10</sup> In the present case, the combination of BSN and KSLA led to computing costs of only about \$3 per structure. This constitutes a reduction by 1-2 orders of magnitude compared to conventional theoretical techniques.<sup>10</sup> The approximations used here yield this computational advantage at little cost in accuracy, especially when kinetic energies  $E$  well above 10 eV are used. For the purpose of structural determination, these approximations give rise to uncertainties that are no larger than the uncertainties inherent in the more accurate conventional methods due to the muffin-tin model of the atomic potential, the homogeneous damping model, and the use of Debye-Waller factors.<sup>11</sup>

While the KSLA scheme has been tested successfully before in several cases<sup>5,11,12</sup> we still need to justify its use in the present situation. KSLA's requirement of negligible intermolecular multiple scattering is certainly well-satisfied by hydrocarbon molecules that are kept separated at van der Waals distances between their respective hydrogen atoms, since the hydrogens do not scatter appreciably: this has been verified previously without BSN<sup>11</sup> and in the course of this work with BSN. When hydrogen atoms are not available as "cushions" between molecules to keep the carbon atoms far apart, a small amount of intermolecular multiple scattering can occur. We have previously observed<sup>12</sup> this to induce errors in the structural determination of less than 0.1 Å (in the case of a layer of close-packed adsorbed CO molecules). The hydrogen cushions of our present structure, therefore, should ensure a good accuracy.

We have applied  $R$  factors to evaluate the level of agreement between theoretical intensities  $I_t$  and experimental intensities  $I_e$  for the various structural modes. We have used the following five  $R$  factors together with their average, as in our initial study of this structure<sup>5</sup> and of many other molecular adsorbate structures:<sup>11-13</sup> ROS = fraction of energy range with slopes of opposite signs in the experimental and theoretical  $I$ - $V$  curves,  $R1 = 0.75 \int |I_e - cI_t| dE / \int |I_e| dE$ ,  $R2 = 0.5 \int (I_e - cI_t)^2 dE / \int I_e^2 dE$ ,  $RRZJ = 0.5 \int ||I_e'' - cI_t''| |I_e' - cI_t'| / (|I_e'| + \max |I_e'|) dE / (0.027 \int |I_e| dE)$ , and  $RPE = 0.5 \int (Y_e - Y_t)^2 dE / \int (Y_e^2 + Y_t^2) dE$ ,  $Y(E) = L / (1 + V_{oi}^2 L^2)$ , where  $L = I'/I$ .

Here  $c = \int |I_e| dE / \int |I_t| dE$  and an apostrophe denotes differentiation with respect to the energy.  $RRZJ$  is the reduced Zanazzi-Jona  $R$  factor, while  $RPE$  is Pendry's  $R$  factor, both renormalized with a factor 0.5 to match the scale of the other  $R$  factors ( $V_{oi}$  is an estimate of the imaginary part of the inner potential, here 4 eV). We shall mainly use the average over these five  $R$  factors, but we shall also quote 2  $RRZJ$  and 2  $RPE$  to allow comparison with other work.

**2.3. Adsorption Structures Tested.** The number of potentially correct structures for  $C_6H_6$  and CO coadsorbed on Rh(111), even within a given two-dimensional unit cell, is enormous. Since in a LEED intensity analysis all potentially correct structures must be tested, we rely on additional information obtained by non-LEED techniques to narrow down the possibilities. Recent thermal desorption spectroscopy experiments<sup>8</sup> imply the following: (1) The majority of the adsorbed benzene molecules are intact at the temperature of the LEED experiment, because the hydrogen desorption characteristic of benzene breakup is not seen. (2) In the  $(\frac{3}{1})$  structure, there is an equal number of benzene and CO molecules, corresponding to about  $\frac{1}{8}$  of a monolayer of each (here 1 monolayer corresponds to 1 adsorbate molecule for each surface metal atom; in these units, benzene saturates the surface at about  $\frac{1}{6}$  of a monolayer and CO saturates the surface at about  $\frac{3}{4}$  of a monolayer; CO coverages are calibrated with known ordered structures of CO adsorbed by itself, while benzene coverages are quoted based on the number of benzene molecules that can fit

(2) Colquhoun, H. M.; Holton, J.; Thompson, D. J.; Twigg, M. V. In *New Pathways for Organic Syntheses*; Plenum: New York, 1984; p 105.

(3) (a) Gentle, T. M.; Muetterties, E. L. *J. Phys. Chem.* **1983**, *87*, 2469. (b) Tysoe, W. T.; Nyberg, G. L.; Lambert, R. M. *J. Chem. Soc., Chem. Commun.* **1983**, 623. (c) Sesselman, W.; Woratschek, B.; Ertl, G.; Küppers, J. *Surf. Sci.* **1983**, *130*, 245.

(4) Parker, W. L.; Hexter, R. M.; Siedle, A. R. *J. Am. Chem. Soc.* **1985**, *107*, 4584.

(5) Van Hove, M. A.; Lin, R. F.; Somorjai, G. A. *Phys. Rev. Lett.* **1983**, *51*, 778.

(6) The general notation ( $m\sqrt{3} \times n$ )rect indicates a rectangular unit cell with sides  $m\sqrt{3}$  and  $n$  times as long as the ( $1 \times 1$ ) unit cell sides; the prefix "c" means "centered".

(7) Lin, R. F.; Koestner, R. J.; Van Hove, M. A.; Somorjai, G. A. *Surf. Sci.* **1983**, *134*, 161.

(8) Mate, C. M.; Somorjai, G. A. *Surf. Sci.* **1985**, *160*, 542.

(9) Van Hove, M. A.; Somorjai, G. A., unpublished results.

(10) Van Hove, M. A.; Tong, S. Y. *Surface Crystallography by LEED*; Springer: Heidelberg, 1979.

(11) Van Hove, M. A.; Somorjai, G. A. *Surf. Sci.* **1982**, *114*, 171.

(12) Van Hove, M. A.; Koestner, R. J.; Frost, J. C.; Somorjai, G. A. *Surf. Sci.* **1983**, *129*, 482.

(13) Koestner, R. J.; Van Hove, M. A.; Somorjai, G. A. *Surf. Sci.* **1981**, *107*, 439.

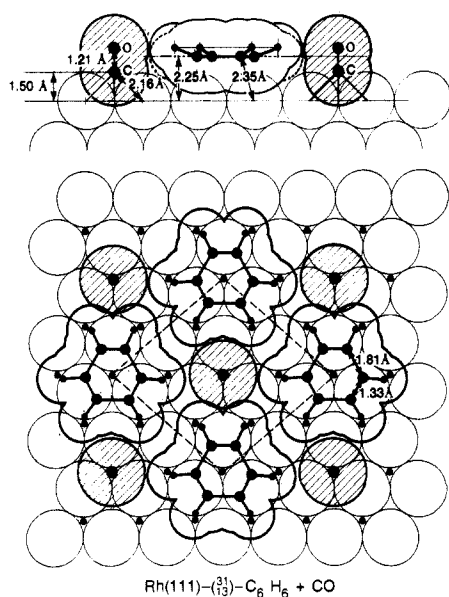


**Figure 1.** Structure of Rh(111)- $(\frac{1}{3})_1$ -C<sub>6</sub>H<sub>6</sub> + CO in side view and top view, including van der Waals contours with radii 1.8 Å for C in benzene, 1.6 Å for C and O in CO, and 1.2 Å for H (the H positions are assumed, including possible CH bending away from the surface). The CO molecules are shown hatched. A  $(\frac{1}{3})_1$  unit cell is outlined. Dots between surface metal atoms denote second-layer metal atoms.

flat in the observed unit cell). Further high-resolution electron energy loss spectroscopy experiments<sup>8</sup> imply the following: (1) The benzene molecules are not only confirmed to be intact but also lie parallel to the surface, rather than being bonded to the metal through their periphery. (2) The presence of CO is responsible for the  $(\frac{1}{3})_1$  unit cell, implying its presence within the unit cell, rather than in a disordered manner. (3) The C-O stretch frequency is such that the CO molecules are most likely bonded with 3-fold coordination to the metal surface, i.e., in hollow sites.

These results indicate that each  $(\frac{1}{3})_1$  unit cell contains one CO molecule ( $\sim 1/8$  of a monolayer) in addition to a single flat-lying benzene molecule. The vacancy left between benzene molecules has the right size to accommodate this single CO molecule, but only if one assumes the particular benzene orientation about its axis shown in Figure 1. Because of steric hindrance between CO and benzene, the two molecules must be centered on the same kind of adsorption site, e.g., hcp-type hollow sites for both molecules, as illustrated in Figure 1.

We have made LEED intensity calculations for a single upright-standing CO molecule and a single flat-lying benzene molecule (with the orientation of Figure 1) in each unit cell for four different registries, i.e., four different high-symmetry adsorption sites: top, bridge, and both kinds of hollow sites (hcp hollow and fcc hollow). In the CO molecules, the CO bond axis was fixed perpendicularly to the surface and the C-O bond length was varied between 1.15 and 1.25 Å (the C-O bond length varies by less than 0.1 Å from one adsorption site to another in metal-carbonyl clusters<sup>14</sup> and on surfaces<sup>12</sup>). The heights of the two molecules above the metal substrate were varied independently of each other. The metal substrate was kept bulklike: significant substrate distortions are unlikely, based on results for other molecular adsorbates on Rh(111).<sup>12,13</sup>

In a first stage of the structural determination, the carbon ring was given its gas-phase geometry (hexagonal symmetry with equal C-C bond lengths of 1.397 Å) and the C-O bond had its gas-phase value of 1.15 Å. This allows the adsorption sites and molecular heights to be approximately determined. Then, in the favored hcp-hollow site, the benzene ring was given a wide range of Kekulé distortions, i.e., alternating long and short C-C bonds. Simultaneously, the heights of the two molecules over the metal surface

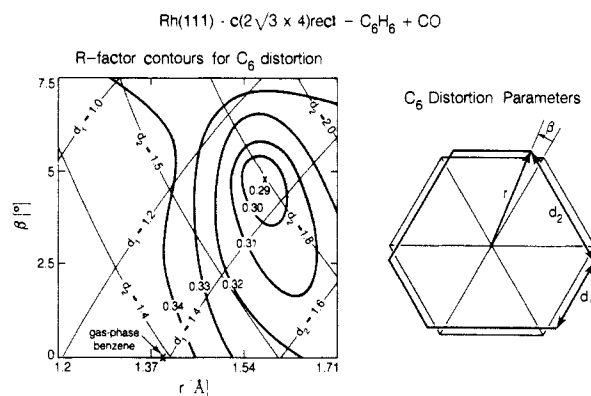


**Figure 2.** Contour plot (left) of the five-*R*-factor average as a function of C<sub>6</sub>-ring distortion in Rh(111)- $(\frac{1}{3})_1$ -C<sub>6</sub>H<sub>6</sub> + CO. The distortion is parametrized by the ring radius *r* and the angular deviation  $\beta$  relative to a hexagon. These parameters are defined at the right, together with the C-C bond lengths *d*<sub>1</sub> and *d*<sub>2</sub>, whose corresponding values are given at the left as contour lines. Other structural parameters are for the optimal geometry given in the text and shown in Figure 1 (except C-O bond length = 1.15 Å and metal-C spacing = 1.45 Å for CO molecules).

were still varied, but with a constant mutual height difference. Without CO, out-of-plane bucklings of the carbon ring have been tested and found to be very unlikely, while a large Kekulé distortion was already observed.<sup>5</sup>

Kekulé distortions involve atomic motions parallel to the surface. We found our LEED analysis to be relatively sensitive to such displacements. We tentatively ascribe this to our large data base, which includes many beams emerging at far off-normal angles. Because many LEED analyses do not share this feature, and because of the potential importance of such distortions, further tests of the optimal Kekulé-type structure were performed: the analysis was repeated with different relative heights of the benzene and CO, with different values of the topmost Rh-Rh interlayer spacing, with the number of phase shifts increased from 5 to 6, with matrix inversion as opposed to a perturbation expansion for the multiple scattering within the molecules, with different values of the muffin-tin zero level (varied at the *R*-factor stage), with individual as opposed to averaged *R* factors, and with *R*-factor comparisons involving subsets of the available beams. Under all these modifications, the optimal atomic positions changed by less than 0.1 Å, both perpendicular and parallel to the surface. Finally, with a fixed benzene distortion, the C-O bond length was varied, as well as the mutual height difference between the two molecules. This resulted in minor corrections, and therefore the structural search was stopped at that stage. In all, about 440 different coadsorption geometries were examined by LEED in this work, in addition to about 960 structures reported<sup>5</sup> in our initial work without CO.

### 3. Results

Our best structure for Rh(111)- $(\frac{1}{3})_1$ -C<sub>6</sub>H<sub>6</sub> + CO, i.e., the structure which minimizes the *R* factors, is illustrated in Figure 1 (the H positions are guessed). In this structure, both benzene and CO occupy hcp-type hollow sites in a compact arrangement. The benzene carbon ring has a spacing of  $2.25 \pm 0.05$  Å to the metal surface with six identical Rh-C bond lengths of  $2.35 \pm 0.05$  Å. The substantial Kekulé-type distortion is evidenced in the *R*-factor contour plot shown in Figure 2: C-C bond lengths alternate between  $1.33 \pm 0.15$  and  $1.81 \pm 0.15$  Å, the short bonds lying over the top of single metal atoms. Such a structure respects the local binding-site symmetry, which is C<sub>3p</sub>( $\sigma_d$ ). This benzene structure is very similar to our previously published structure for this system, obtained by ignoring the CO coadsorption.<sup>5</sup>

The optimal metal-carbon interplanar spacing for CO in our structure is  $1.50 \pm 0.05$  Å, corresponding to a Rh-C bond length of  $2.16 \pm 0.04$  Å. The best C-O bond length is found to be  $1.21 \pm 0.05$  Å.

The optimal structure has values of the Zanazzi-Jona *R* factor, Pendry *R* factor, and five-*R*-factor average of 0.40, 0.66, and 0.31,

(14) Chini, P.; Longoni, G.; Albano, V. G. *Adv. Organomet. Chem.* **1976**, *14*, 285.

respectively (these values can vary by  $\pm 0.10$ ,  $\pm 0.10$ , and  $\pm 0.03$ , respectively, as the theoretical method is changed). The best muffin-tin zero level, a nonstructural parameter which is optimized at the same time as all the structural parameters, is  $8 \pm 1$  eV below vacuum.

#### 4. Discussion

**4.1. Coadsorption-Induced Ordering.** A notable occurrence in the coadsorption of benzene and CO on Rh(111) is the mutual reordering of the two species, i.e., the change of each other's long-range periodicity. It is known that neither pure benzene overlayers nor pure CO overlayers produce a  $\left(\frac{31}{13}\right) = c(2\sqrt{3} \times 4)\text{rect}$  periodicity on Rh(111). Indeed, benzene without CO orders, at saturation coverage, in a  $(2\sqrt{3} \times 3)\text{rect}$  structure,<sup>8</sup> and CO without benzene orders in  $(\sqrt{3} \times \sqrt{3})R30^\circ$ <sup>13</sup> or  $(2 \times 2)^{12}$  structures, depending on the coverage. Furthermore, increasing the CO coverage to  $\sim 2/9$  of a monolayer in the presence of  $\sim 1/9$  of a monolayer of benzene yields a  $(3 \times 3)$  coadsorption structure<sup>7,8</sup> (compared with  $1/8$  of a monolayer of CO and  $1/8$  of a monolayer of benzene in the  $\left(\frac{31}{13}\right)$  structure). Here, the coverage values have been idealized to indicate their relationship with the unit cell sizes of nine Rh atoms and eight Rh atoms, respectively.

This example of ordering modified by coadsorption illustrates a general phenomenon: coadsorption can be used to modify long-range order. One can even create long-range order when there was none, as in the case of CO added to benzene on Pt(111).<sup>8</sup> Similar behavior has been encountered for CO coadsorbed with other adsorbates, such as ethylidyne, methylacetylene, propylidyne, chloro- and fluorobenzene, and sodium, on Rh(111), as well as with NO rather than CO as a coadsorbate on Rh(111).<sup>15</sup> The added variety of structures due to coadsorption helps solve surface structures by providing more closely related test cases. Especially helpful is the situation where a disordered overlayer is induced to order, simplifying the structural determination. Such closely related structures can exhibit differences in chemical bonding, which in turn can contribute to chemical understanding, as we shall illustrate next. Clearly, one must beware of the possibility of gross structural differences, which, in the case of adsorbed molecules, can easily be detected by HREELS.

**4.2. Adsorption Sites.** It appears that the equilibrium adsorption site of both benzene and CO is modified by their coadsorption. For CO this is firmly established: without benzene or other coadsorbates, CO adsorbs in either 1-fold coordinated top sites or (above  $1/3$  of a monolayer coverage) also in 2-fold coordinated bridge sites but never in 3-fold coordinated hollow sites, as is known from HREELS and LEED.<sup>12,13,16a</sup> Our finding of a hollow site for CO in the presence of benzene is the first crystallographic evidence for hollow site occupation by CO on any metal surface. The recent HREELS measurements for this system already suggested this site,<sup>8</sup> based on the empirical relationship between CO stretch frequency and site occupation found in metal-carbonyl clusters.<sup>16b</sup> This relationship states that when the C-O stretch frequency falls in the (approximate) ranges 1650–1850, 1850–2000, or 2000–2150  $\text{cm}^{-1}$ , the CO molecule is adsorbed respectively in a 3-, 2-, or 1-fold coordinated site. Our result is the first confirmation of that empirical relationship for CO in hollow sites on surfaces.

Hollow site occupation by CO on several metal surfaces, including Rh(111), has also been suggested when CO is coadsorbed with potassium or other alkali metals.<sup>17</sup> There, a mechanism of charge transfer from potassium to CO via the metal substrate has

**Table I.** Rh-C Bond Lengths for Adsorbed CO (Å)

	3-fold hollow	2-fold bridge	1-fold top
surfaces	$2.16 \pm 0.04^a$	$2.03 \pm 0.07^b$	$1.94 \pm 0.1^{b,c}$
complexes	2.17–2.23 <sup>d</sup>	2.00–2.09 <sup>d</sup>	1.82–1.91 <sup>d</sup>

<sup>a</sup>This work. <sup>b</sup>Reference 12. <sup>c</sup>Reference 13. <sup>d</sup>Reference 14.

been proposed. By analogy, with benzene substituted for potassium, a similar mechanism can be proposed involving charge donation by the benzene  $\pi$ -ring orbitals (these are the molecular orbitals most involved in the bonding to the metal surface). This would be consistent with the known electron-donating character of benzene, as detected by work function measurements.<sup>18,18</sup>

The effect of CO on the benzene adsorption site is less well-established because no LEED intensity analysis of the CO-free benzene structure has been performed. However, the observed  $(2\sqrt{3} \times 3)\text{rect}$  structure of pure benzene on Rh(111) appears to possess glide-plane symmetry,<sup>8</sup> which can best be explained by bridge-site adsorption (a full LEED intensity analysis of this structure is in preparation). If a site change from bridge to hollow is indeed induced by CO, presumably the same charge-transfer mechanism from benzene to CO mentioned above could be held responsible: the presence of CO would withdraw more charge from benzene, causing a site change. However, the assignment of a benzene adsorption site based on the HREEL spectra is not fully resolved at this stage, despite extensive work.<sup>17,18,19</sup>

**4.3. CO Bond Lengths.** The Rh-C bond length for CO is found to be  $2.16 \pm 0.04$  Å in the hollow site. This is compared in Table I with values for bridge and top sites on rhodium surfaces and in small rhodium-carbonyl complexes. A good correspondence is observed, which gives additional confidence in the overall structure determination. Note the clear site dependence of the metal-C bond length: it increases markedly on moving from 1- to 2- to 3-fold coordination. This is true both in metal-carbonyl complexes and for CO adsorbed at metal surfaces.

The C-O bond length is found to be  $1.21 \pm 0.05$  Å, which is expanded by  $0.06 \pm 0.05$  Å with respect to the gas-phase value. This result may be compared with a similar expansion of the C-O bond by  $0.12 \pm 0.03$  Å for CO coadsorption with Na on Pt(111), as detected by NEXAFS<sup>17f</sup> (where the CO adsorption site is also likely to be a 3-fold hollow site and the molecular axis is near to the surface normal). A C-O bond lengthening is in line with the observed bond weakening, as measured by HREELS,<sup>8</sup> which takes place also with coadsorbed alkali metals.<sup>17</sup> Specifically, the C-O stretch frequency measured by HREELS for CO/Na/Pt(111)<sup>17f</sup> is  $1690 \text{ cm}^{-1}$ , while for our structure of CO/C<sub>6</sub>H<sub>6</sub>/Rh(111)<sup>8</sup> it is  $1655 \text{ cm}^{-1}$ , compared with  $2143 \text{ cm}^{-1}$  in the gas phase.

**4.4. Structure of Benzene Adsorbed on the Rh(111) Surface.** We find a strong distortion of the benzene ring, with alternating long and short C-C bonds that match the symmetry of the 3-fold adsorption site: the resulting species may be called 1,3,5-cyclohexatriene. The carbon-ring radius is also considerably increased with respect to gas-phase benzene ( $1.58 \pm 0.15$  vs.  $1.397$  Å). Our estimated error bars of  $\sim 0.15$  Å (based on *R*-factor contour plots like that of Figure 2) and our various tests described above are such that we have confidence in the presence of a distortion of this order of magnitude.

The only result which is at variance with our conclusions is that of Neumann et al.:<sup>18</sup> they find 6-fold rather than 3-fold symmetry of benzene adsorbed on Rh(111), by ARUPS.

A number of organometallic complexes exist with which we may compare our result: these involve various aromatics or other cyclic molecules, including benzene,<sup>20</sup> tri- and hexamethylbenzene,<sup>21</sup> cyclopentadiene,<sup>22</sup> and azulene.<sup>23</sup> These molecular

(15) Proceedings of Vibrations at Surfaces IV: Mate, C. M.; Bent, B. E.; Somorjai, G. A. *J. Electron Spectrosc. Relat. Phenomena*, in press; and unpublished results.

(16) (a) Dubois, L. H.; Somorjai, G. A. *Surf. Sci.* **1980**, *91*, 514. (b) Eischens, R. P.; Pliskin, W. *Adv. Catal.* **1958**, *10*, 1.

(17) (a) Crowell, J. E.; Garfunkel, E. L.; Somorjai, G. A. *Surf. Sci.* **1982**, *121*, 303. (b) Crowell, J. E.; Somorjai, G. A. *Appl. Surf. Sci.* **1984**, *19*, 73. (c) Hoffmann, F. M.; de Paola, R. A. *Phys. Rev. Lett.* **1984**, *52*, 1967. (d) Lee, J.; Hanrahan, C. P.; Arias, J.; Martin, R. M.; Metiu, H. *Phys. Rev. Lett.* **1983**, *51*, 1803. (e) Ruckenstein, E.; Halachev, T. *Surf. Sci.* **1982**, *122*, 422. (f) Sette, F.; Stöhr, J.; Kollin, E. B.; Dwyer, D. J.; Gland, J. L.; Robbins, J. L.; Johnson, A. L. *Phys. Rev. Lett.* **1985**, *54*, 935.

(18) Gland, J.; Somorjai, G. A. *Surf. Sci.* **1973**, *38*, 157.

(19) Waddill, G. D.; Kesmodel, L. L., unpublished results.

(20) (a) Gomez-Sal, M. P.; Johnson, B. F. G.; Lewis, J.; Raithby, P. R.; Wright, A. H. *J. Chem. Soc., Chem. Commun.* **1985**, 1682. (b) Wismer, V., Ph.D. Thesis, University of Bochum, West Germany, 1981. (c) Allegra, G.; Tettamanti Casagrande, G.; Immirzi, A.; Porri, L.; Vitulli, G. *J. Am. Chem. Soc.* **1970**, *92*, 289. (d) Nardin, G.; Delise, P.; Allegra, G. *Gazz. Chim. It.* **1975**, *105*, 1047.

species normally bond through their  $\pi$ -orbitals to the metal atoms, i.e., such that the metal atoms lie against the flat side of the molecules, usually centered close to the ring axis (alternatively, metal atoms may substitute for peripheral H atoms). We are aware of only two complexes in which benzene has been determined<sup>20a</sup> to be faced-bonded to three metal atoms, mimicking an fcc(111) site: they are  $\text{Ru}_3\text{C}(\text{CO})_{11}(\text{C}_6\text{H}_6)_2$  and  $\text{Os}_3(\text{CO})_9(\text{C}_6\text{H}_6)$ , hereinafter referred to as complexes I and II.

Our Rh-C bond length of  $2.35 \pm 0.05 \text{ \AA}$  is in good agreement with metal-C bond lengths in those complexes. In particular, for complexes I and II, the (averaged) metal-carbon bond lengths are 2.27 and 2.32  $\text{Å}$ , respectively.

The complexes I and II exhibit a clear Kekulé distortion of the benzene ring which is very similar to that found by us on Rh(111): it has the same 3-fold symmetry and also features short C-C bonds over individual metal atoms and long C-C bonds bridging two metal atoms. For complexes I and II, the (averaged) short C-C bond lengths are 1.39 and 1.40  $\text{Å}$ , while the (averaged) long C-C bond lengths are 1.48 and 1.48  $\text{Å}$ , respectively; these values are to be compared with our stronger Kekulé distortion values of  $1.33 \pm 0.15$  and  $1.81 \pm 0.15 \text{ Å}$ . The various complexes<sup>20-23</sup> show relatively small deviations from the C-C distance of 1.397  $\text{Å}$  in gas-phase benzene. This is typical of organometallic clusters. The largest C<sub>6</sub>-ring distortion in a complex which we have found in the literature concerns bis(hexamethylbenzene)ruthenium(0),<sup>21a</sup> with sequential C-C distances of 1.327, 1.498, 1.480, 1.408, 1.415, and 1.487  $\text{Å}$  (this particular ring does not have 3-fold symmetry; in fact it is strongly bent toward the "boat" shape of cyclohexane). A strong Kekulé distortion occurs for hexamethylbenzene-tri-carbonylmolybdenum,<sup>21b</sup> with sequential C-C distances of 1.399, 1.431, 1.408, 1.444, 1.407, and 1.448  $\text{Å}$ , i.e.,  $\sim 0.04\text{-}\text{Å}$  variation compared with our  $\sim 0.48 \text{ Å}$ . All these examples also exhibit the general trend of a ring expansion, but not as large as ours, which increases the carbon-ring radius from 1.397 to  $\sim 1.58 \text{ Å}$ .

Long C-C bonds are not uncommon in organic molecules in the gas phase. Many examples of C-C bond lengths in excess of 1.60  $\text{Å}$  are found in the literature<sup>24,25</sup> (the conventional C-C single bond length is 1.54  $\text{Å}$ ). The largest values which we know of<sup>25</sup> are 1.780-1.851  $\text{Å}$  in the molecules 11,11-dimethyltricyclo-[4.4.1.0<sup>1,6</sup>]undeca-2,4,7,9-tetraene and 11-methyltricyclo-[4.4.1.0<sup>1,6</sup>]undeca-2,4,7,9-tetraene-11-carbonitrile. A long C-C bond is usually explained as resulting from a conformational strain that pulls the two carbon atoms apart. This situation may apply in our surface system as well, if we assume that the closely bonded C-C pairs of a benzene molecule attempt to move apart. The driving force could be provided by repulsive H-H interactions or more favorable adsorption sites for these ethylenic (H-C=C-H) species.

Note that substantial out-of-plane distortions are common for aromatics in small organometallic complexes, because the aromatics attempt to wrap themselves around the metal cores or bind off-center. By contrast, in our case on Rh(111), as in the complexes I and II, there is no reason for an out-of-plane distortion of the carbon ring, given the binding site symmetry (the benzene hydrogens however are likely to bend out of plane due to the rehybridization around the carbons, as we shall discuss below). A substantial out-of-plane distortion would in any case be readily detected by HREELS. This has been illustrated by the observation

with HREELS of tilts away from parallelism with the surface for  $\text{C}_6\text{H}_5\text{Cl}$ ,<sup>26</sup>  $\text{C}_6\text{H}_5\text{F}$ ,<sup>26</sup>  $\text{C}_5\text{H}_5\text{N}$ ,<sup>26</sup> and  $\text{C}_5\text{H}_6$ ,<sup>1c</sup> and no tilts for  $\text{C}_6\text{H}_6$ <sup>1f,8,19</sup> and  $\text{C}_5\text{H}_5$ <sup>1e</sup> on various metal surfaces.

Recently, the adsorption of benzene<sup>27,28</sup> and related aromatics<sup>29</sup> on metal surfaces has been modeled theoretically. The complexity of the computational problem led to the use of versions of the Extended Hückel theory. These calculations did not include coadsorbed CO. The substrates were Rh(111)<sup>28,29</sup> and Ni, Ag and Pt(111),<sup>27</sup> modeled as clusters of 3 to 17 metal atoms<sup>27-29</sup> or as periodic surfaces in the tight-binding model.<sup>28</sup> The preferred adsorption site appears to be a 3-fold hollow site on each metal, but the bridge site is energetically close. It is thus quite plausible that CO coadsorption could induce a site change of benzene, as we seem to observe on Rh(111) upon addition of CO. In the hollow site, the same benzene orientation about its axis was found as with LEED: half the C-C bonds lie above individual rhodium atoms; this corresponds to  $C_{3v}(\sigma_h)$  symmetry (cf. Figure 1). The calculations also seem to give a slight preference for the hcp-hollow site over the fcc-hollow site.<sup>27</sup>

The theoretical metal-carbon bond lengths are in reasonable agreement with the LEED results: 2.15  $\text{Å}$  by Extended Hückel theory vs.  $\sim 2.35 \text{ Å}$  from LEED, on Rh(111). Regarding the benzene geometry, the major adsorption effect predicted by the theory is a C-H bond bending away from the surface plane by about 20° on Rh(111).<sup>28</sup> This cannot be directly tested by LEED, but it would at least be compatible with the carbon positions found by LEED. It also matches well the observation that the out-of-plane C-H bending vibration is the mode which changes its HREELS frequency most upon adsorption.<sup>1f</sup> Theory also predicts a substantial ring expansion<sup>28</sup> by about 0.12  $\text{Å}$ , compared with the LEED result of about 0.18  $\text{Å}$ . The largest theoretical Kekulé-type distortion yielded<sup>28</sup> alternating C-C bond lengths of 1.50 and 1.64  $\text{Å}$ . Whatever the numerical values, a clear tendency toward C-C bond length expansion is found. This is consistent with the LEED result and with previous observations of reductions in the C-C bond order for other adsorbed unsaturated hydrocarbons, such as acetylene ( $\text{C}_2\text{H}_2$ )<sup>30-32</sup> and ethylene ( $\text{C}_2\text{H}_4$ ).<sup>31,33</sup> For instance, with NEXAFS,<sup>31</sup> bond lengthening to  $1.45 \pm 0.03$  and  $1.49 \pm 0.03 \text{ Å}$ , respectively, is observed for acetylene and ethylene on Pt(111), compared to gas-phase values of 1.20 and 1.33  $\text{Å}$ . One would expect such a tendency due to the formation of metal-carbon bonds upon adsorption and the resulting rehybridization around the carbon atoms. Associated with the C-C bond-order reduction in benzene is a C-C bond weakening, which is evidenced by a frequency reduction in HREELS.<sup>1f</sup> Note that the theory finds no evidence for C-H bond weakening, so that C-C bond scission is the easier decomposition pathway. The distortion seen in LEED suggests in a different way the same conclusion.

**4.5. Benzene and Acetylene Interconversion.** The observed strong distortion of benzene on Rh(111) corresponds more to a 1,3,5-cyclohexatriene species than to benzene. Although the benzene appears to have nearly decomposed into three adsorbed ethylenic (H-C=C-H) species, we have several experimental pieces of evidence to confirm that the molecules have not fully transformed to independent  $\text{C}_2\text{H}_2$  species. These include the observation by HREELS of ring-vibration modes and the observation by TDS that the benzene molecules are still intact at temperatures up to  $\sim 400 \text{ K}$ ,<sup>8</sup> well above the decomposition temperature of acetylene ( $\sim 270 \text{ K}$ ).<sup>34</sup> It is, however, significant

(21) (a) Hüttner, G.; Lange, S. *Acta Crystallogr., Sect. B* **1972**, *B28*, 2049. (b) Koshland, D. E.; Myers, S. E.; Chesick, J. P. *Acta Crystallogr., Sect. B* **1977**, *B33*, 2013.

(22) Mills, O. S.; Shaw, B. W. *J. Organomet. Chem.* **1968**, *11*, 595.

(23) Churchill, M. R.; Gold, K.; Bird, P. H. *Inorg. Chem.* **1969**, *8*, 1956.

(24) Many early examples are given in: Hounshell, W. D.; Dougherty, D. A.; Hummel, J. P.; Mislow, K. *J. Am. Chem. Soc.* **1977**, *99*, 6. And in ref 30 therein. More recent examples are given in: Hisatome, M.; Kawaziri, Y.; Yamakawa, K.; Iitaka, Y. *Tetrahedron Lett.* **1979**, *20*, 1777. Littke, W.; Drück, U. *Angew Chem.* **1979**, *91*, 434. Dougherty, D. A.; Schlegel, H. B.; Mislow, K. *Tetrahedron* **1978**, *34*, 1441. Harano, K.; Ban, T.; Yasuda, M.; Osawa, E.; Kanematsu, K. *J. Am. Chem. Soc.* **1981**, *103*, 2310. Osawa, E.; Ivanov, P. M.; Jaime, C. *J. Org. Chem.* **1983**, *48*, 3990.

(25) (a) Bianchi, R.; Morosi, G.; Mugnoli, A.; Simonetta, M. *Acta Crystallogr., Sect. B* **1973**, *B29*, 1196. (b) Bianchi, R.; Pilati, T.; Simonetta, M. *Acta Crystallogr., Sect. B* **1978**, *B34*, 2157.

(26) Mate, C. M.; Somorjai, G. A., unpublished results.

(27) Anderson, A. B.; McDevitt, M. R.; Urbach, F. L. *Surf. Sci.* **1984**, *146*, 80.

(28) Minot, C.; Garfunkel, E. L.; Gavezzotti, A.; Simonetta, M. *Surf. Sci.*, in press.

(29) Gavezzotti, A.; Ortoleva, E.; Simonetta, M. *Chem. Phys. Lett.* **1983**, *98*, 536.

(30) Ibach, H.; Lehwald, S. *J. Vac. Sci. Technol.* **1978**, *15*, 407.

(31) Stöhr, J.; Sette, F.; Johnson, A. L. *Phys. Rev. Lett.* **1984**, *53*, 1684.

(32) Wang, P.-K.; Slichter, C. P.; Sinfelt, J. H. *Phys. Rev. Lett.* **1984**, *53*, 82.

(33) Ibach, H.; Mills, D. L. *Electron Spectroscopy for Surface Analysis*; Academic: New York, 1982.

that benzene is much more likely to decompose than to desorb as the temperature is raised (only about 2% desorb intact):<sup>8</sup> this indicates that the tightly bound benzene will more likely distort and break its  $\pi$ -ring stabilization than remain intact. Also, coadsorption of potassium, a net electron donor, decreases the likelihood of decomposition, at least on Pt(111).<sup>35</sup> Therefore, we may tentatively propose that coadsorption of CO, a net electron acceptor, would enhance the decomposition of benzene by favoring distortion. Furthermore, a detailed analysis<sup>36</sup> of the benzene decomposition products upon heating on Rh(111) (namely -CH and -CCH species) favors acetylene as an intermediate product, even if short-lived.

Rh, unlike Pd, does not catalyze the conversion of acetylene to benzene. Whereas such a reaction has been observed on Pd(111),<sup>3</sup> it was not seen on the Rh(111) single-crystal surface. It is, however, most encouraging that the benzene-to-acetylene conversion appears to have been observed recently for the first time:<sup>4</sup> indeed, Raman spectroscopy detected acetylene formation after benzene adsorption on supported Rh particles in the presence of coadsorbed CO in an ultra-high vacuum cell.

Hopefully, structural results such as ours for benzene on Rh(111) and others in preparation on Pt(111) and Pd(111) will help clarify the mechanisms of this reaction.

## 5. Conclusions

We have made the first structural analysis of a molecular coadsorbate system. It is characterized by mutual ordering and

site shifting of the coadsorbate species, benzene and CO. We have found the first confirmed hollow-site adsorption of CO on a single-crystal surface, with bond lengths that are quite consistent with comparable bond lengths in metal-carbonyl clusters.

The benzene is also hcp-hollow-sited and its carbon ring exhibits a strong Kekulé-type distortion and an expansion. This result may be connected with the mechanisms of acetylene-benzene interconversion reactions on metal catalysts.

We have recently also analyzed<sup>37</sup> the Rh(111)-(3 × 3)-C<sub>6</sub>H<sub>6</sub> + 2CO system with LEED intensities. It differs from the Rh(111)-(3<sub>13</sub>)-C<sub>6</sub>H<sub>6</sub> + CO system described here mainly in the presence of two rather than one CO molecules per unit cell. The structural results are essentially identical: hcp hollow sites for benzene and CO and the same Kekulé distortion for benzene. The optimal numerical values for the bond lengths are somewhat different: short and long C-C bond lengths of 1.48 ± 0.15 and 1.58 ± 0.15 Å, respectively. This agreement, using totally independent LEED data bases, gives additional confidence in our results.

**Acknowledgment.** We are grateful for helpful discussions with C. M. Mate, E. L. Garfunkel, C. Minot (made possible by a NATO joint travel grant), A. Gavezzotti, M. Simonetta (made possible by a NSF-CNR joint travel grant), and A. B. Anderson, as well as for a literature search by C. T. Kao. This work was supported by the Director, Office of Energy Research, Office of Basic Energy Sciences, Materials Science Division, of the U.S. Department of Energy under Contract DE-AC03-76SF00098. Supercomputer time was also provided by the Office of Energy Research of the Department of Energy.

Registry No. C<sub>6</sub>H<sub>6</sub>, 71-43-2; CO, 630-08-0; Rh, 7440-16-6.

(37) Koestner, R. J.; Lin, R. F.; Blackman, G. S.; Kao, C. T.; Van Hove, M. A.; Somorjai, G. A., unpublished results.

(34) Dubois, L. H.; Castner, D. G.; Somorjai, G. A. *J. Chem. Phys.* **1980**, *72*, 5234.

(35) Garfunkel, E. L.; Maj, J. J.; Frost, J. C.; Farias, M. H.; Somorjai, G. A. *J. Phys. Chem.* **1983**, *87*, 3629. Crowell, J. E., Ph.D. Thesis, University of California, 1984.

(36) Koel, B. E.; Crowell, J. E.; Bent, B. E.; Mate, C. M.; Somorjai, G. A., unpublished results.

# Gas-Phase Photodissociation of FeCH<sub>2</sub><sup>+</sup> and CoCH<sub>2</sub><sup>+</sup>: Determination of the Carbide, Carbyne, and Carbene Bond Energies

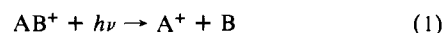
R. L. Hettich and B. S. Freiser\*

Contribution from the Department of Chemistry, Purdue University, West Lafayette, Indiana 47907. Received August 16, 1985

**Abstract:** Photodissociation of MCH<sub>2</sub><sup>+</sup> (M = Fe, Co) is observed to yield three products M<sup>+</sup>, MC<sup>+</sup>, and MCH<sup>+</sup>. This result is in contrast to the low-energy collision-induced dissociation of MCH<sub>2</sub><sup>+</sup>, which yields M<sup>+</sup> exclusively. From the photoappearance thresholds of the products, the following bond energies are assigned:  $D^{\circ}(\text{Co}^+-\text{CH}_2) = 84 \pm 5$  kcal/mol,  $D^{\circ}(\text{Co}^+-\text{CH}) = 100 \pm 7$  kcal/mol,  $D^{\circ}(\text{Co}^+-\text{C}) = 90 \pm 7$  kcal/mol,  $D^{\circ}(\text{Fe}^+-\text{CH}_2) = 82 \pm 5$  kcal/mol,  $D^{\circ}(\text{Fe}^+-\text{CH}) = 101 \pm 7$  kcal/mol, and  $D^{\circ}(\text{Fe}^+-\text{C}) = 94 \pm 7$  kcal/mol. Compared to the results of an earlier ion-beam study, the Co<sup>+</sup>-CH<sub>2</sub> bond energy reported here is in excellent agreement while the Fe<sup>+</sup>-CH<sub>2</sub> value is significantly lower.

The transition metal-ligand chemical bond has been described as being the key to linking organometallic chemistry, surface chemistry, and catalysis.<sup>1</sup> In particular, metal-ligand bond energies provide a means of assessing whether a proposed reaction pathway is energetically feasible. We recently reported that photodissociation shows promise as a method for obtaining this information,<sup>2</sup> complementing the growing number of theoretical<sup>3</sup> and experimental<sup>4</sup> techniques.

In order for an ion to photodissociate, process 1, first the ion



must absorb a photon, second the photon energy must exceed the enthalpy for the reaction, and third the quantum yield for photodissociation must be non-zero.<sup>5,6</sup> Because of these requirements, thresholds observed in the photodissociation spectrum are governed

(1) Schaefer, H. F., III *Acc. Chem. Res.* **1977**, *10*, 287.  
(2) Cassady, C. J.; Freiser, B. S. *J. Am. Chem. Soc.* **1984**, *106*, 6176.  
(3) (a) Alvarado-Swaigood, A. E.; Allison, J.; Harrison, J. F. *J. Phys. Chem.* **1985**, *89*, 2517. (b) Shim, I.; Gingerich, K. A. *J. Chem. Phys.* **1982**, *77*, 2490. (c) Harris, J.; Jones, R. O. *J. Chem. Phys.* **1979**, *70*, 830.

(4) (a) Armentrout, P. B.; Beauchamp, J. L. *J. Am. Chem. Soc.* **1981**, *103*, 784. (b) Ervin, K.; Loh, S. K.; Aristov, N.; Armentrout, P. B. *J. Phys. Chem.* **1983**, *87*, 3593. (c) Morse, M. D.; Smalley, R. E. *Ber. Bunsenges. Phys. Chem.* **1984**, *88*, 228. (d) Murad, E. *J. Chem. Phys.* **1983**, *78*, 6611.

(5) Freiser, B. S.; Beauchamp, J. L. *J. Am. Chem. Soc.* **1976**, *98*, 3136.  
(6) Orth, R. G.; Dunbar, R. C. *J. Am. Chem. Soc.* **1982**, *104*, 5617.